Acta Chemica Scandinavica, 1996: 50: 275–283
Printed in Belgium – all rights reserved

ACTA
CHEMICA SCANDINAVICA
ISSN 0904–213X

Syntheses and Crystal Structures of Titanium Oxide Sulfates

M. A. K. Ahmed, H. Fjellvåg and A. Kjekshus†

Department of Chemistry, University of Oslo, N-0315 Oslo, Norway

Ahmed, M. A. K., Fjellvåg, H. and Kjekshus, A., 1996. Syntheses and Crystal Structures of Titanium Oxide Sulfates. – Acta Chem. Scand. 50: 275–283

When titanium dioxide, metatitanic acid or iron titanate (ilmenite) is heated with 65–95 wt% H_2SO_4, $TiOSO_4$ or $TiOSO_4 \cdot H_2O$ is formed depending on the water content of the sulfuric acid. The contours of reaction mechanisms are discussed. $TiOSO_4$ and $TiOSO_4 \cdot H_2O$ dissolve slightly in cold or hot water during short-term treatment. On longer contact with water the solubility becomes more appreciable. The undissolved remainder, as well as the dissolved fraction after removal of the water phase, proves to have been converted into X-ray amorphous products with composition $TiOSO_4 \cdot xH_2O$, $x \approx 1$. The crystal structure of $TiOSO_4$ [orthorhombic, $a = 1095.3(3)$, $b = 515.2(1)$ and $c = 642.6(1)$ pm] has been determined on the basis of powder X-ray diffraction data. The structure of $TiOSO_4 \cdot H_2O$ has been redetermined. Both structures contain ...–O–Ti–... zigzag chains with short Ti–O distances. The chains are connected via sulfate groups, and the structures probably suffer from some disorder. For both structures the possibility of deviations from the centrosymmetric space group *Pnma* is discussed. The close structural relationship between $TiOSO_4$ and $TiOSO_4 \cdot H_2O$ is discussed. On heating, $TiOSO_4$ undergoes a reversible phase transition at around 330 °C and decomposes into TiO_2-a (anatas) at ca. 525 °C. $TiOSO_4 \cdot H_2O$ looses its crystal water at ca. 310 °C. However, liberation of SO_3 starts at about 40 °C lower temperature than for $TiOSO_4$, and the decomposition shows a two-step character in TG, DTG and DTA. Attempts to isolate intermediate decomposition product(s) have so far not been successful.

The use of concentrated H_2SO_4 (in this context 60–95 wt% H_2SO_4) as a solvent has long traditions in pure and industrial chemistry. Nevertheless, reactions in and with conc. H_2SO_4 are little systematically explored and understood. It can not be denied that working with conc. H_2SO_4 has certain disadvantages, some of which are of a psychological nature owing to the risk of damaging living organisms or materials coming into contact with the acid. The high viscosity, some 25 times that of water, introduces experimental difficulties: solutes dissolve and crystallize more slowly, adhered H_2SO_4 may be difficult to remove from the reaction product and concentration fluctuations may be present. However, for many purposes the advantages of conc. H_2SO_4 may be more important: extreme acidobasic differentiating power combined with weakly developed redox properties. Its dielectric constant is higher than that of water, making it a good solvent for ionic substances and leading to extensive autoionization.

The situation for titanium oxide sulfate, $TiOSO_4$, may serve to illustrate the points mentioned above. $TiOSO_4$ and/or its hydrates are dealt with in textbooks,[1] reference books,[2] original[3–6] and patent[7] literature, and are also involved in industrial processes for the manufacture of titanium compounds (cf. Ref. 2 and references therein). Yet limited completely reliable information on the titanium oxide sulfates is available apart from the crystal structure determination of $TiOSO_4 \cdot H_2O$,[4] and the approximate unit-cell dimensions for $TiOSO_4$.[6] The present work, which has its origin in interest in gaining insight into the numerous possible reactions in conc. H_2SO_4 (cf. Ref. 8), will hopefully contribute to rectifing this situation.

Experimental

TiO_2 {Aldrich; >99.9%, anatase [TiO_2-a, $a = 378.41(3)$, $c = 951.2(2)$ pm]}, ilmenite (Egersund, Norway; pure mineral specimen of $FeTiO_3$) and conc. H_2SO_4 (Merck; 95–97 wt%, the former value being used throughout this paper) were used as starting chemicals for the syntheses. Concentrated H_2SO_4 in the range 60–95 wt% H_2SO_4 was made by diluting the as-purchased acid with distilled H_2O. Owing to the virtually lacking reactivity of the as-purchased TiO_2-a in 60 wt% H_2SO_4, a parallel series of syntheses made use of metatitanic acid (cf. Refs. 2–4) as

† To whom correspondence should be addressed.

an intermediate in a two-step reaction. [In the first step, metatitanic acid was obtained: TiO_2 was dissolved in H_2SO_4 (*vide infra*), the solution cooled to room temperature, whereafter conc. NH_3 was added slowly under cooling until the liquid became weakly basic. The resulting deposit was then filtered, carefully washed, dried, crushed, and washed and dried once more. The metatitanic acid thus obtained ($TiO_2 \cdot xH_2O$) was virtually X-ray amorphous (am)].

Four parallel series of syntheses were performed, using either the as-purchased TiO_2-a, the rutile [TiO_2-r; $a = 459.30(5)$ and $c = 295.63(5)$ pm] modification (converted from TiO_2-a at 1000°C), $FeTiO_3$ (ilmenite) or $TiO_2 \cdot xH_2O$-am as the titanium oxide source. TiO_2 or $FeTiO_3$ (0.02 mol) was added to 20 ml conc. H_2SO_4 (60–95 wt%) in a round-bottomed flask with either a glass stopper (90–95 wt% H_2SO_4) or a reflux cooler (60–85 wt% H_2SO_4). The mixtures were heated to boiling under stirring until all titanium oxide material (for the successful syntheses) had dissolved, and a clear yellow to dark-brown solution was obtained. The stirring was then stopped, but the heating was continued. After a few minutes (up to 30 min) with clear solution, the liquid turned cloudy and a white precipitate began to deposit. The heating was maintained for another 5 min before being stopped. During the cooling and the storing at room temperature, the precipitation continued. The reaction vessel was kept untouched until the precipitate was well separated from the H_2SO_4 mother liquor. The liquid phase was removed by decantation, the precipitate was transferred to a beaker containing ca. 100 ml of glacial acetic acid, stirred for 10 min, filtered off, washed with acetic acid, acetone, diethylether and dried in a desiccator.

All samples were characterized by powder X-ray diffraction (PXD) using Guinier–Hägg cameras, Cr $K\alpha_1$ or Cu $K\alpha_1$ radiation and Si as internal standard. High-temperature PXD data were collected with a Guinier–Simon camera (Enraf–Nonius) between 20 and 500°C at a heating rate of 25°C h^{-1}. The samples were contained in open silica-glass capillaries. The positions of the Bragg reflections were obtained from the films by means of a Nicolet L18 scanner using the SCANPI program system.[9] The diffraction pattern of $TiOSO_4$ was indexed with the help of the TREOR program.[10] Unit-cell dimensions were obtained from least-squares refinements using the CELLKANT program.[11]

PXD intensity data for the crystal structure determination and/or refinements of $TiOSO_4$ and $TiOSO_4 \cdot H_2O$ were collected with a Siemens D500 diffractometer, using monochromatic Cu $K\alpha_1$ radiation. The data were recorded in steps of 0.02° in 2Θ between 10 and 110°, and the counting time for each setting was 30 s; flat plate in reflection mode geometry (Bragg–Brentano), 1 and 1° slits in front of the sample, 1 and 0.18° in front of the scintillation counter. The fine powders were pressed into a standard sample holder. In addition, powder neutron diffraction data for $TiOSO_4$ were collected with the OPUS III two-axis diffractometer at the JEEP II reactor, Kjeller. Data corrections, deconvolution, structure determination and profile refinements were performed with the ALLHKL,[12] SIRPOW[13] and DBW3.2S[14] programs.

Differential scanning calorimetry (DSC) measurements were made between 20 and 600°C with a Mettler TA 3000 system. Open Al_2O_3 crucibles were used for the 15–25 mg samples, nitrogen was used as atmosphere and the heating/cooling rate was 5–10°C min^{-1}. Thermogravimetric (TG) and differential thermal (DTA) analyses were performed between 20 and 1000°C with a Perkin Elmer TGA 7 and DTA 7 system, respectively. The 15–25 mg samples were placed in Al_2O_3 crucibles, nitrogen was used as an atmosphere and the heating rate was 10°C min^{-1}.

Results and discussion

(i) Synthesis of $TiOSO_4$ and $TiOSO_4 \cdot H_2O$. The progressing reactions between TiO_2-a/r, $TiO_2 \cdot xH_2O$-am or $FeTiO_3$ and 65–95 wt% H_2SO_4 are evidenced by the dissolution of the solids and the colouring of the liquid phase. No detectable reaction was found for any of the solid reactants in 60 wt% H_2SO_4. The fact that two-phase mixtures of $TiOSO_4$ and $TiOSO_4 \cdot H_2O$ are obtained in the intermediate concentration range around 75 wt% H_2SO_4 (Table 1) is attributed to kinetics. In line with the polymeric nature of the Ti–O framework in $TiOSO_4$ and $TiOSO_4 \cdot H_2O$ (see ii), these compounds are very difficult to redissolve in H_2SO_4 once they are formed.

As seen from Table 1, $TiOSO_4$ and $TiOSO_4 \cdot H_2O$ are the only solid compounds obtained from TiO_2-a/r and $TiO_2 \cdot xH_2O$-am in 65–95 wt% H_2SO_4. Hence, the exist-

Table 1. Products resulting from the reaction of TiO_2-a/r, $TiO_2 \cdot xH_2O$-am or $FeTiO_3$ (ilmenite) with 60–95 wt % H_2SO_4. Yields for TiO_2-a/r series are 85–95% of the calculated amount and for $TiO_2 \cdot xH_2O$-am series some 30%, whereas yields are not determined for $FeTiO_3$ series.

"TiO_2" reactant	Wt % H_2SO_4							
	60	65	70	75	80	85	90	95
TiO_2-a/r	N.r.[a]	$TiOSO_4 \cdot H_2O$ →		Two-phase[b]	$TiOSO_4$ →			
$TiO_2 \cdot xH_2O$-am	N.r.[a]	$TiOSO_4 \cdot H_2O$ →			Two-phase[b]	$TiOSO_4$ →		
$FeTiO_3$	N.r.[a]	N.t.[c]	U.p.[d] →			$TiOSO_4$[e] →		

[a] No reaction. [b] Mixture of $TiOSO_4$ and $TiOSO_4 \cdot H_2O$. [c] Not tested. [d] Unidentified products. [e] Also for 84 wt %.

ence of $TiOSO_4 \cdot 2H_2O$ claimed in Refs. 2, 3 and 5 could not be confirmed by our method. The findings concur, on the other hand, with Refs. 4, 6 and 7. The yields of the syntheses are very good (85–95% of the calculated amount) when TiO_2-a/r is used as reagent, but decrease generally with decreasing concentration of sulfuric acid. With $TiO_2 \cdot xH_2O$-am as reactant, the yields become much poorer (some 30%).

$TiOSO_4$ and $TiOSO_4 \cdot H_2O$ were characterized by PXD (see Refs. 4 and 6 and Section ii). Their compositions were verified by quantitative chemical analysis (S determined as $BaSO_4$; for $TiOSO_4$, obs. 20.5% S, calc. 20.01 wt%; for $TiOSO_4 \cdot H_2O$, see Ref. 4), from the crystal structure determinations (see Ref. 4 and Section ii) and from TG measurements (see Section iv).

The course of the reaction between TiO_2-a/r and H_2SO_4 has certain features (a period with a clear, light-yellow coloured solution followed by rapid precipitation of the polymerized product) in common with that[8] between Bi, I_2O_5 and H_2SO_4. This leads us to postulate a three-step reaction mechanism:

$$TiO_2(s) + H_2SO_4 \rightarrow TiO^{2+}(solv) + SO_4^{2-}(solv) + H_2O(solv) \quad (1)$$

followed by the polymerization:

$$n TiO^{2+}(solv) \rightarrow (TiO)_n^{2n+}(solv) \quad (2)$$

and finally the precipitation:

$$(TiO)_n^{2n+}(solv) + n\, SO_4^{2-}(solv) \rightarrow n\, TiOSO_4(s) \quad (3)$$

The reaction with $FeTiO_3$ proceeds almost certainly quite similarly; however, the presence of the iron component prevents ascertainment of the colouring of the solution resulting from step (1). A very dark colouring is a distinguishing mark when $TiO_2 \cdot xH_2O$-am rather than TiO_2-a/r is used as reactant in combination with the most concentrated sulfuric acid solutions studies (black for 95 wt% H_2SO_4: virtually colourless at 70 wt% H_2SO_4). The essential difference between $TiO_2 \cdot xH_2O$-am and TiO_2-a/r (and $FeTiO_3$) is the amorphous state of the former. The amount of water introduced from $TiO_2 \cdot xH_2O$-am is considered too small to play a major role. On this basis we suggest that the dark colour represents intermediately sized $(TiO)_n^{2n+}(solv)$ species, say, with n of the order of 10 and with different configurations of the ...–Ti–O–... chains than when formed according to the steps (1) and (2).

When $TiOSO_4$ and $TiOSO_4 \cdot H_2O$ are treated with cold or hot 60–95 wt% H_2SO_4, H_2O or 1 M NH_3 for a short period of time, no or very limited solubility is observed, and water may in fact be used as washing agent. Similar behaviour is observed for cold 1 M HCl and 1 M H_2SO_4, whereas both compounds are readily dissolved when treated with hot, diluted acids.

When $TiOSO_4$ and $TiOSO_4 \cdot H_2O$ are kept in contact with H_2O at room temperature for a prolonged time, the solubility proves to be more appreciable, with a saturation value of ca. 1 g dissolved in 100 ml H_2O after one week with intermediate stirrings. The thus obtained diluted aqueous solutions of $TiOSO_4$ are colourless, but on gradual evaporation the colour turns yellowish and finally a distinctly yellow, transparent, glassy material is obtained. The crushed, off-white powder obtained from the glassy material appears X-ray amorphous. On heating the yellowish glassy material at 150 °C, it turns into a nearly black glassy material. Probably the colour change is introduced by the changed disorder consequent on removal of included water. At first sight it is surprising that the undissolved, major remains after $TiOSO_4$ and $TiOSO_4 \cdot H_2O$ (white powders) are also converted into amorphous materials after prolonged contact with water. However, the complete conversion of the bulk phase is merely a consequence of the equilibrium situation between dissolved and undissolved titanium oxide sulfate. The converted bulk product shows no colour change on heating.

On heating (see also Section iv), the amorphous products, here termed $TiOSO_4 \cdot xH_2O$-am, gradually give off included and crystal water, and at some 350 °C (according to fixed temperature experiments, not observed by DSC) a major dehydration occurs together with crystallization of $TiOSO_4$.

(ii) Crystal structure determination and refinements. The crystal structure of $TiOSO_4$ was solved from scratch on the basis of PXD data. (The combined single crystal and PXD determination of unit-cell dimensions and probable space group for $TiOSO_4$ was pointed out to us by one of the referees. However, both the unit-cell dimensions and the indexing in Ref. 6 are slightly, yet significantly, incorrect.)

Data from Guinier photographs were subjected to trial-and-error indexing by the TREOR program.[10] This gave an orthorhombic unit cell with the dimensions $a = 1095.3(3)$, $b = 515.2(1)$ and $c = 642.6(1)$ pm [$V = 362.6(2) \times 10^6$ pm^3; all (32) reflections indexed; figure of merit[15] $M(20) = 21$].

The (probable) systematic extinctions in the PXD data, $0kl$ absent when $k + l = 2n + 1$ and $hk0$ absent when $h = 2n + 1$, leaves a choice between the space groups *Pnma* and *Pn2$_1$a*. Both space groups were tested out during the structure refinements, see below. The observed density, 2.89 ± 0.04 g cm^{-3} at 25.00 ± 0.01 °C, shows that the unit-cell content is four ($Z_{obs} = 3.95$) $TiOSO_4$ formula units.

The observed PXD profiles (Fig. 1) were deconvoluted by means of the ALLHKL program,[12] and the obtained set of F_{obs}^2 was, together with unit-cell dimensions, space group and unit-cell content used as input parameters for the direct methods program SIRPOW.[13] This treatment gave a proposal for the crystal structure of $TiOSO_4$ with very reasonable coordinates for titanium and sulfur, but with various possible locations for the four non-equiva-

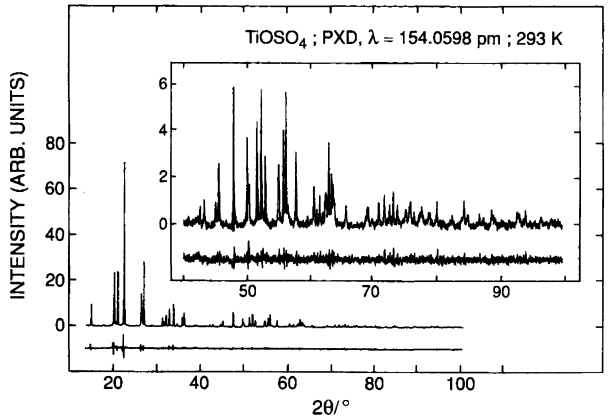

Fig. 1. Observed and difference (observed − calculated) PXD profiles for $TiOSO_4$.

lent oxygen atoms. At this stage, the observed PXD pattern was subjected to Rietveld analysis by the program DBW3.2S[14] with parameters for the trial structure, the scale factor, the counter zero point and the half-width parameters (pseudo-Voigt function) as variables. From variation of occupation numbers, the correct choice for the location of oxygen atoms was settled, and the structure determination was continued with regular least squares Rietveld refinements (246–257 reflections, 4000–5000 data points, 27 variables). At this stage, bond valence[16] calculations (see Section iii) suggested that certain details were not completely resolved. For this reason, PND data were collected and refined, but without providing more satisfactory bond valence data (for both Ti and S).

Four means to modify the data analyses were tried in order to identify possible sources for the non-satisfactory results; taking the possibility of preferred orientation into account, removal of the (small) low-angle part of the PXD diagram with very strong reflections, turning to anisotropic description of the atoms with the largest temperature factors, and refinements in the non-centrosymmetric space group $Pn2_1a$ (No. 33). In accordance with the fact that the samples of $TiOSO_4$ and $TiOSO_4 \cdot H_2O$ were agglomerates of very small particles, introduction of preferred orientation parameters had no significant effects on the refinements. Excluding the region 10–30° in 2Θ (i.e. shutting out 11 reflections; Fig. 1) gave minor improvements. Turning to an anisotropic temperature factor description for the atoms O(1) and O(4), which could simulate disorder for these atoms, gave hardly any significant improvement in terms of reliability factors, but gave atomic coordinates which in turn resulted in somewhat more reasonable bond valences (see Section iii). For the refinements according to the non-centrosymmetric space group $Pn2_1a$, the O(1) atoms, which occupy an eight-fold position according to *Pnma*, were split in two four-fold positions, whereas all other parameters were constrained at the values prescribed by *Pnma*. As a next step, the y-parameters were entered as variables (y_{Ti} fixed at 0.25). However, the improvements in the reliability factors were not significant, and hence $Pn2_1a$ hardly provides any better description of the structure than *Pnma*. The observed and difference (observed − calculated) plots for the PXD profiles in Fig. 1 leave no doubt that the main features are well described according to the higher symmetric space group. The resulting final values for the positional parameters according to *Pnma* are listed in Table 2. On the other hand, the use of anisotropic temperature factor descriptions for O(1) and O(4) gave large B_{22} components which may indicate that the true symmetry is lower than concluded here (see also Ref. 6).

Although the crystal structure of $TiOSO_4 \cdot H_2O$ reported in Ref. 4 appears to be correct to a large extent, it needs refinement for three reasons. First, there is a space group ambiguity in that Ref. 4 claims that the real symmetry is $P2_12_12_1$, yet the refinements are performed according to *Pnma*. Second, the refinements in Ref. 4 kept some of the variable oxygen parameters effectively fixed. Third, the large scatter in the S–O distances (124–157 pm) and the improbable Ti and S valences which follow from the Ti–O and S–O distances are in themselves good reasons for renewed refinements.

The present refinements of the $TiOSO_4 \cdot H_2O$ structure were carried out for PXD data collected for a sample synthesized from $TiO_2 \cdot xH_2O$-am and 65 wt% H_2SO_4 (Section i). The obtained unit-cell data $a = 982.8(1)$, $b = 513.4(1)$, $c = 861.3(1)$ pm and $V = 434.6(2) \times 10^6$ pm^3 are in fair agreement with results presented in Ref. 4. The refinements were carried out as described for $TiOSO_4$ (297–309 reflections, 4000–5000 data points; 30–34 variables). For $TiOSO_4 \cdot H_2O$, the removal of the region 10–30° in 2Θ reduced R_{wp} from 14.8 to 10.8. Also for $TiOSO_4 \cdot H_2O$, problems with unexpected large deviations

Table 2. Positional parameters and temperature factors with calculated standard deviations in parentheses for the crystal structure of $TiOSO_4$ as derived form PXD data [space group *Pnma*, 246 reflections, $R_p = 6.72$, $R_{wp} = 8.66$, goodness of fit, $GOF = 1.72$; see text concerning anisotropic temperature factor description for O(1) and O(4)].

Atom	Position	x	y	z	$B_{iso}/10^4$ pm^2
Ti	4*c*	0.5593(3)	1/4	0.6636(5)	1.4(2)
S	4*c*	0.8435(4)	1/4	0.4778(7)	1.8(2)
O(1)	8*d*	0.8662(8)	0.4922(22)	0.3621(19)	3.0(3)
O(2)	4*c*	0.7097(9)	1/4	0.5243(22)	2.8(2)
O(3)	4*c*	0.9108(8)	1/4	0.6709(17)	2.8(3)
O(4)	4*a*	0	0	0	2.4(2)

Table 3. Positional parameters with calculated standard deviations in parentheses for the crystal structure of $TiOSO_4 \cdot H_2O$ as derived form PXD data [space group *Pnma*, 300 reflections, $R_p = 7.74$, $R_{wp} = 10.60$, goodness of fit, $GOF = 2.41$; see text concerning anisotropic temperature factor description for O1(1) and O(4); $B_{iso} = (0.4–0.6) \times 10^4$ pm^2 for Ti and S, $(0.5–1.5) \times 10^4$ $pm^2$for O]. Corresponding values from Ref. 4 are included (below) for comparison. Numbering of atoms follows Ref. 4.

Atom	Position	*x*	*y*	*z*
Ti	4*c*	0.1258(2)	1/4	0.9574(3)
		0.125	1/4	0.963
S	4*c*	0.6743(3)	1/4	0.1654(5)
		0.679	1/4	0.155
O(1)	4*a*	0	0	0
		0	0	0
O(2)	4*c*	0.5258(8)	1/4	0.1362(11)
		0.553	1/4	0.151
O(3)	4*c*	0.2164(7)	1/4	0.1691(10)
		0.221	1/4	0.168
O(4)	8*d*	0.2686(12)	0.5064(16)	0.9045(14)
		0.26	0.51	0.91
O(5)	4*c*	0.5821(7)	1/4	0.7704(8)
		0.572	1/4	0.763

in calculated valences were found (Section iii). More satisfactory distances were achieved by adopting anisotropic temperature factors for O(1) and O(4) (viz. compensating some kind of structural disorder or symmetry reduction by giving large B_{22} and B_{11} components, respectively). Slight such improvements were further achieved for refinements according to the non-centrosymmetric space group $Pn2_1a$ where the eight-fold position is split up in two four-fold positions. Introduction of more free variables (e.g. *y*-parameters according to $Pn2_1a$ or $P2_12_12_1$ as suggested by Lundgren[4]) was considered meaningless on the basis of the quality of the present data. In summary, it is concluded that the most correct picture is presently achieved by adopting *Pnma* and an anisotropic temperature factor description for O(1) and O(4) (Table 3). Attention should be drawn to the fact that the reaction mechanism (Section i) which rules the syntheses of these compounds makes it quite likely that there exists some disorder between sulfate groups in $TiOSO_4$ as well as between sulfate and/or water groups in $TiOSO_4 \cdot H_2O$.

(iii) A closer look at the crystal structures of $TiOSO_4$ and $TiOSO_4 \cdot H_2O$. Relevant interatomic distances in the crystal structures of $TiOSO_4$ and $TiOSO_4 \cdot H_2O$ are listed in Table 4, and projections and perspective views of the structures are shown in Fig. 2. The infinite ...–Ti–O–... zigzag chains, which are very distinctive features of both structures, run horizontally (along ***b***) in the projections. The interchain Ti–O distances are about of equal length, 179 pm in $TiOSO_4$ versus 182 pm $TiOSO_4 \cdot H_2O$. These distances are notably very short compared with the expected value for a normal Ti–O bond (around 195 pm). The structures contain slightly distorted tetrahedral SO_4 groups (S–O distances of 144–150 pm in $TiOSO_4$ and 148–150 pm in $TiOSO_4 \cdot H_2O$) as can easily be recognized in Fig. 2. In $TiOSO_4$ the oxygen atoms of the SO_4 groups are connected to four different titanium atoms at distances of 188–201 pm. In $TiOSO_4 \cdot H_2O$ only three of the oxygen atoms of the SO_4 group are bonded to titanium atoms at distances of 198–203 pm. The fourth oxygen atom of the SO_4 group, O(2), is directed towards the open channel where the water molecules are found (Fig. 2D). In this channel, the six oxygen–oxygen distances between the oxygen of the water molecule and surrounding oxygens [O(1), O(2) and O(4)] are around 270–290 pm, which are in the typical range for O···H–O hydrogen bonds in hydrates.

The details of the actual structures (Fig. 2) tend to blur the essential differences between $TiOSO_4$ and $TiOSO_4 \cdot H_2O$. Therefore, simplified and idealized projective representations of the two structures are given in Fig. 3, which immediately focuses the attention on the different arrangement of the ...–Ti–O–... chains. In $TiOSO_4$ (Fig. 3A) the chains run completely parallel, whereas they are related by mirror imaging in $TiOSO_4 \cdot H_2O$ (Fig. 3B; the relation may alternatively be described as displacement along the chain direction between successive chains). The different ways of joining the SO_4 groups to the ...–Ti–O–... chains is a result of the different chain arrangements and the incorporated crystal water in $TiOSO_4 \cdot H_2O$.

Despite the close structural relationship between $TiOSO_4$ and $TiOSO_4 \cdot H_2O$, the structural changes which are involved in converting one into the other of these compounds must be classified as major. The removal of crystal water from $TiOSO_4 \cdot H_2O$ is easily accomplished through thermal decomposition (onset at ca. 340°C, Section iv), but the rather rough treatment introduces additional disorder which causes the obtained $TiOSO_4$ product to perform somewhat differently from that prepared by direct synthesis. Hydratization of $TiOSO_4$ is on the other hand impossible at normal conditions (*inter alia* long-range refluxing in boiling 65 wt% H_2SO_4). The only path from $TiOSO_4$ to $TiOSO_4 \cdot H_2O$ appears to go via decomposition of the former into TiO_2-a/r (or conversion into $TiO_2 \cdot xH_2O$-am) and completely repeated synthesis in 65–75 wt% H_2SO_4 (Section i). The reluctance to allow H_2O to enter the $TiOSO_4$ structure directly is understandable on the basis of the required structural rearrangements.

Figure 3 also serves to bring out structural relationships between $TiOSO_4$, $TiOSO_4 \cdot H_2O$ and $(IO)_2SO_4$ (see Refs. 17 and 18). The dominating feature of the three structures are ...–*X*–O–... zigzag chains. The different connections of the SO_4 groups to the chains may be regarded as reflections of the chemical formulae (or *vice versa*), but notably, iodine is four-coordinated whereas titanium in six-coordinated. The differences in bonding situation and crystal structure are manifested in strikingly different reactivity with water. $(IO)_2SO_4$ undergoes rapid hydrolysis into I_2O_4 when exposed to moisture, whereas $TiOSO_4$ and $TiOSO_4 \cdot H_2O$ are much more water resis-

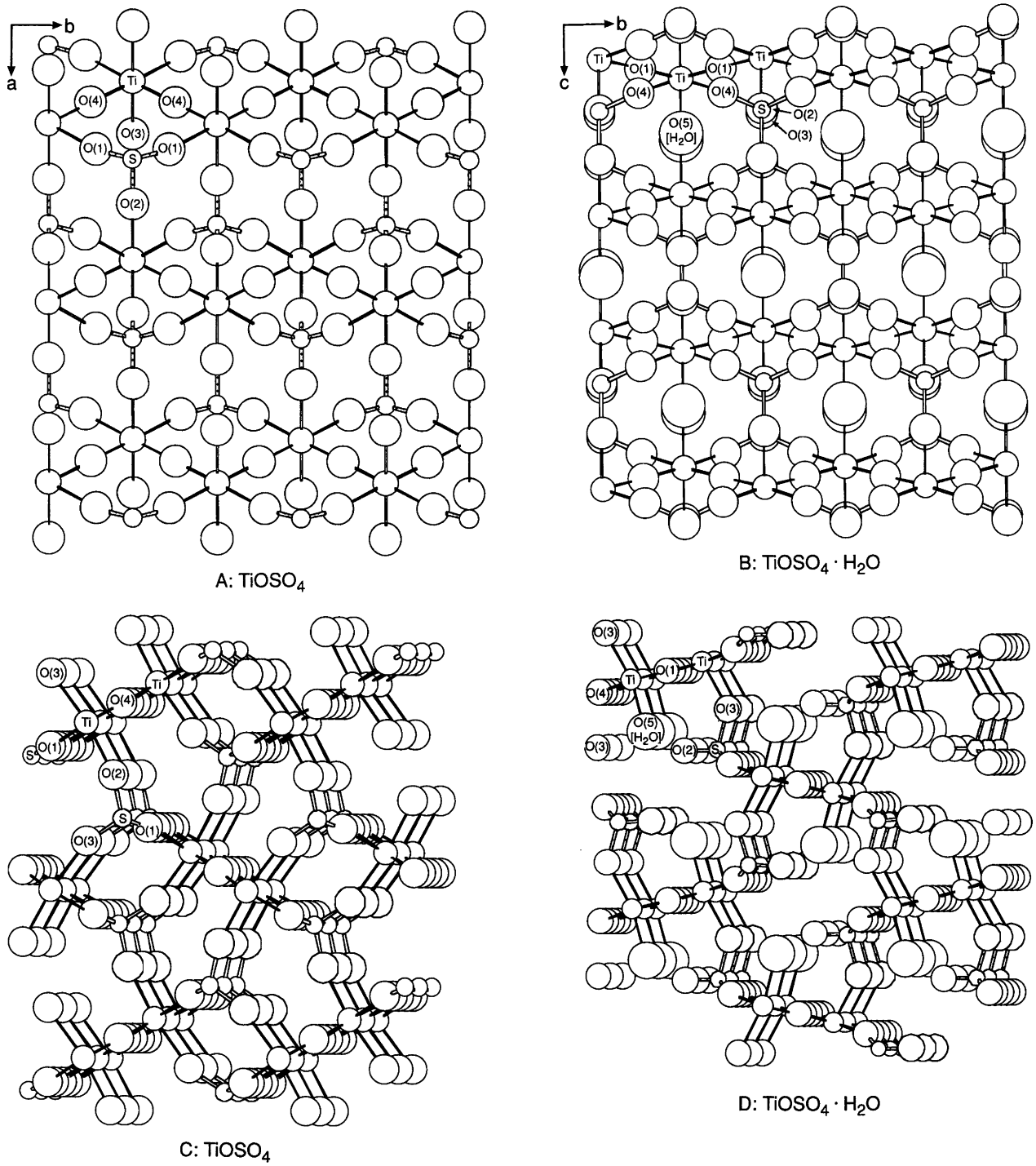

Fig. 2. The crystal structure of (A) $TiOSO_4$ and (B) $TiOSO_4 \cdot H_2O$ projected along [001] and [100], respectively, and in perspective views along [010] for (C) $TiOSO_4$ and (D) $TiOSO_4 \cdot H_2O$. The numbering of crystallographic non-equivalent atoms is shown on the illustrations. Oxygens [O(5)] of the crystal water in B and D are marked by larger circles, hydrogen positions are not determined.

tant (Section i). The sulfates are only the first examples of a large class of compounds comprised of ...–*X*–O–... zigzag chains. Representatives are further found among main group metalloids (e.g. Bi and Te), transition metals (e.g. V), and furthermore, the SO_4 may be exchanged by other anionic groups (e.g. SeO_4 etc.). Compounds like $KTiOPO_4$ and $CsTiOAsO_4$ also have some features in common with the titanium oxide sulfates.[19, 20] Their structures comprise tetrahedral PO_4 and AsO_4 groups, and the titanium atoms are connected in ...–Ti–O–... chains with

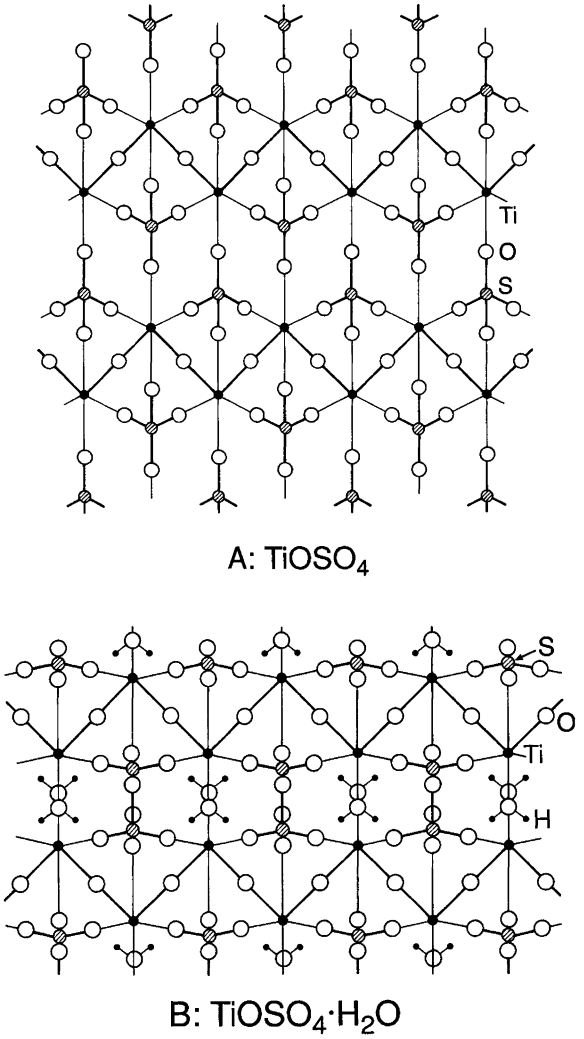

Fig. 3. Simplified and idealized representations of the structures of (A) $TiOSO_4$ and (B) $TiOSO_4 \cdot H_2O$ in the 'same' projections as in Figs. 2A and 2B, respectively.

short Ti–O distances (171.6–173.3 pm for $KTiOPO_4$). $KTiOPO_4$ and $CsTiOAsO_4$ have very interesting non-linear optical properties rooted in their non-centrosymmetric crystal structures (space group $Pna2_1$). The optical properties of $TiOSO_4$ and $TiOSO_4 \cdot H_2O$ are not known, but in view of the space group ambiguities discussed above, they are certainly candidates for an examination.

It may be instructive to calculate bond valencies (V_i) from the observed distances (d_{ij}/100 pm; Table 4) according to the expression:[16]

$$V_i = \sum_j \exp\left[(D_{ij} - d_{ij})/b\right]$$

where D_{ij} is the bond-valence parameter for the particular bond concerned and $b = 0.37$. For Ti^{IV}–O and S^{VI}–O bonds, Ref. 16 lists $D_{ij} = 1.815$ and 1.624, respectively. The calculations gave $V_{Ti-O} = 4.89$ and $V_{S-O} = 6.06$ for $TiOSO_4$ and $V_{Ti-O} = 4.43$ and $V_{S-O} = 5.75$ for $TiOSO_4 \cdot H_2O$, values which deviate unsatisfactory much

Table 4. Interatomic distances (in pm) for the crystal structure of $TiOSO_4$ and $TiOSO_4 \cdot H_2O$.

$TiOSO_4$			
Bonding distances			
Ti–O(1)×2	201.4	S–O(1)×2	147.4
Ti–O(2)	187.6	S–O(2)	149.6
Ti–O(3)	194.4	S–O(3)	144.3
Ti–O(4)×2	178.6		
Shortest distances neglected as bonding			
Ti–O	385	S–O	360
Ti–S	331		
$TiOSO_4 \cdot H_2O$			
Bonding distances			
Ti–O(1)	181.9	S–O(2)	148.1
Ti–O(3)	202.9	S–O(3)	148.4
Ti–O(4)×2	197.7	S–O(4)×2	149.7
Ti–O(5)	202.9		
Shortest distances neglected as bonding			
Ti–O	364	S–O	352
Ti–S	328		

from the expected values of 4 and 6, respectively. The significant discrepancies may either reflect crystal disorder or lower symmetry than used during the refinements (see Refs. 4 and 6).

(iv) Effects of heat treatment on $TiOSO_4$ and $TiOSO_4 \cdot H_2O$. Lundgren[4] made use of the two-step decomposition of $TiOSO_4 \cdot H_2O$ to analyse its composition. In the present study, TG, DTG and DTA have been utilized more systematically to explore the effects of heat treatment on $TiOSO_4$ and $TiOSO_4 \cdot H_2O$.

$TiOSO_4$ represents the simplest case. When single phase, carefully washed and dried $TiOSO_4$ is subjected to TG, a one-step thermal decomposition occurs:

$$TiOSO_4(s) \rightarrow TiO_2(s) + SO_3(g) \qquad (4)$$

(Fig. 4A; onset at 525°C, maximum at ca. 675°C and completion at ca. 720°C for 10°C min^{-1} heating rate and N_2 atmosphere). The observed, relative weight loss, $\Delta m/m_0 = 0.4988$, is in excellent agreement with the calculated value (0.5005) according to eqn. (4). Careful washing and drying is required to achieve such an excellent result, and TG is actually a valuable technique to design optimum conditions for the drying procedure. The final, solid product is TiO_2-a.

Inspection of the DTA curve for $TiOSO_4$ reveals a small, endothermic peak at 320–420°C which has no counterpart in TG. This is caused by a structural phase transition. When heating a $TiOSO_4$ sample at ca. 350°C, the colour turns light lemon yellow, whereas it reverts to white on cooling. This appears to be an effect of the phase transition, and is probably related to charge-transfer ex-

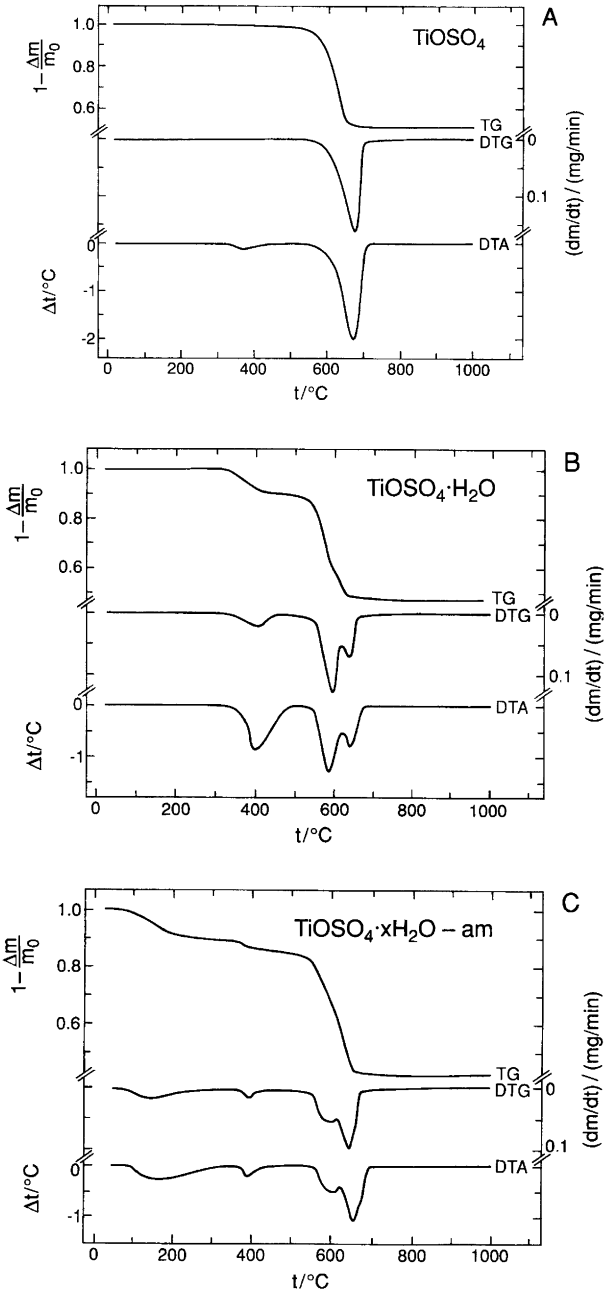

Fig. 4. TG, DTG and DTA data for (A) $TiOSO_4$, (B) $TiOSO_4 \cdot H_2O$ and (C) $TiOSO_4 \cdot xH_2O$. The DTA scans are adjusted to constant background signal.

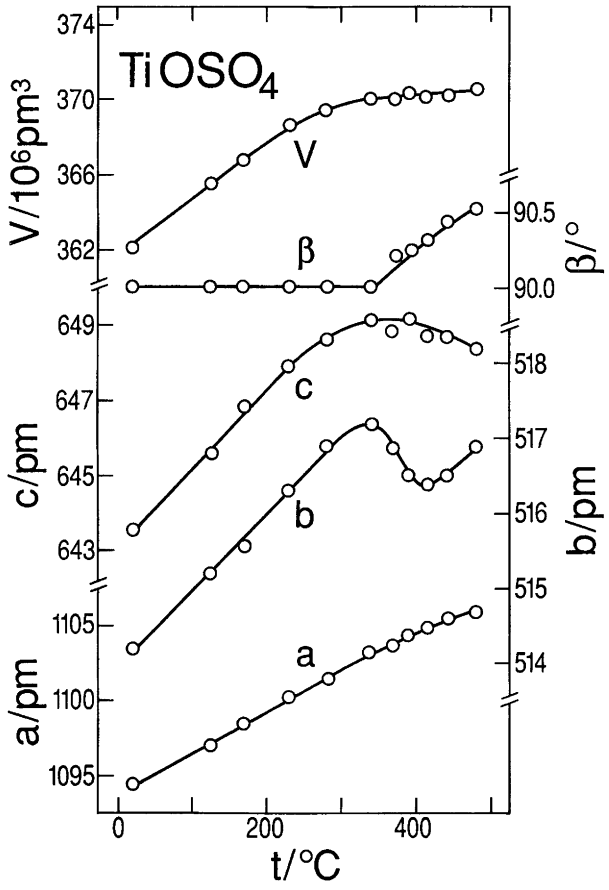

Fig. 5. Variation of unit-cell dimensions with temperature for $TiOSO_4$. Transition $TiOSO_4(I) \rightleftarrows TiOSO_4(II)$ at 350 ± 10°C, decomposition of $TiOSO_4(II)$ at 500 ± 20°C. Thermal expansion coefficients 20–250°C (in 10^{-5} K^{-1}): $\alpha_a = 2.4$, $\alpha_b = 2.0$, $\alpha_c = 2.3$, $\alpha_V = 7.8$. [Thermal expansion coefficients for $TiOSO_4 \cdot H_2O$ at 20–250°C (in 10^{-5} K^{-1}): $\alpha_a = 4.8$, $\alpha_b = 1.9$, $\alpha_c = 0.0$, $\alpha_V = 6.6$.]

citations. High-temperature PXD confirms the transition (cf. the thermal expansion curves for $TiOSO_4$ in Fig. 5), which we denote

$$TiOSO_4(I)(s) \rightleftharpoons TiOSO_4(II)(s) \qquad (5)$$

to emphasize its reversible nature. PXD gave a transition temperature of 350 ± 10°C. The very slight changes in intensities of the Bragg reflections indicate that the structural differences between the modifications are rather minor. However, the distinct line splitting for $TiOSO_4(II)$ clearly proves that the symmetry changes from orthorhombic to monoclinic on heating, which is somewhat surprising for a temperature-induced transition.

TG, DTG and DTA data for a good quality (requires cautious washing and drying) sample of $TiOSO_4 \cdot H_2O$ are shown in Fig. 4B. In comparison to $TiOSO_4$, the monohydrate undergoes the additional decomposition:

$$TiOSO_4 \cdot H_2O(s) \rightarrow TiOSO_4(s) + H_2O(g) \qquad (6)$$

(onset at ca. 310°C, maximum at ca. 400°C and completion at ca. 485°C for 10°C min^{-1} heating rate and N_2 atmosphere). The observed relative weight loss, $\Delta m/m_0 = 0.0997$, is in good agreement with 0.1012 as calculated for the dehydratization reaction (6). The dehydratization of $TiOSO_4 \cdot H_2O$ takes place in the same temperature interval as the phase transition (5) in the anhydrate. Although the overall, observed relative weight

loss ($\Delta m/m_0 = 0.4982$) for the subsequent decomposition of $TiOSO_4$ formed according to reaction (5) into TiO_2-a complies with reaction (4), some essential details differ. First, the onset and completion temperatures in Fig. 4B are lowered by some 40 °C compared with Fig. 4A. Second, and more remarkable, is to find that reaction (4) is composed of two steps in Fig. 4B. The characteristic features of one and two steps decompositions in TG, DTG and DTA were found for all synthesized samples of $TiOSO_4$ and $TiOSO_4 \cdot H_2O$.

The composite character of the $TiOSO_4$ to TiO_2-a reaction in Fig. 4B shows striking resemblance with corresponding recordings for $CuSO_4 \cdot 5H_2O$, where the terminal step from $CuSO_4$ to Cu_2O also occurs in two stages.[21] By careful regulation of the decomposition temperature, the intermediate Cu_2OSO_4 could be successfully isolated.[21] Inspired by Ref. 21, the TG apparatus was used in an attempt to perform analogous partial decomposition of $TiOSO_4$ [formed according to reaction (6)] at 520 °C. However, despite numerous attempts, these experiments have so far not been successful.

TG, DTG and DTA data for $TiOSO_4 \cdot xH_2O$-am are presented in Fig. 4C. The results are chosen for a sample which with luck in washing and drying gave a total weight loss ($TiOSO_4 \cdot xH_2O$ to TiO_2-r) well on the way to matching that in Fig. 4B. Although Figs. 4B and C have features in common, the details differ. $TiOSO_4 \cdot xH_2O$-am starts to loose weight (water) already below 100 °C, and the dehydratization [the analogoue of reaction (6)] goes more or less continuously into the liberation of SO_3 according to reaction (4). The distinct features in Fig. 4B are hence more smeared out in Fig. 4C. The lack of distinct thermoanalytical responses are just as expected when amorphous phases are involved, as is also the observation of a certain degree of irreproducibility between experiments on different samples of $TiOSO_4 \cdot xH_2O$-am.

Acknowledgement. The present work has received financial support from The Research Council of Norway.

References

1. Hägg, G. *General and Inorganic Chemistry*, Almqvist and Wiksell, Stockholm 1969.
2. *Gmelin's Handbuch der anorganischen Chemie, System-Nummer 41: Titan*, Verlag Chemie, Weinheim 1951.
3. Pamfilov, A. V. and Khudyakova, T. A. *Zhur. Obsh. Khim. 19* (1949) 1443, see also *Chem. Abstr. 44* (1950) 1354a.
4. Lundgren, G. *Arkiv Kemi 10* (1956) 397.
5. Reynolds, M. L. and Wiseman, T. J. *J. Inorg. Nucl. Chem. 29* (1967) 1381.
6. Naka, S., Tanaka, K., Suwa, Y. and Takeda, Y. *J. Inorg. Nucl. Chem. 39* (1977) 1239.
7. Kirkham, A. and Spence, H. *Brit. Pat. No. 263886* (1925), compl. accept. 1927 I 2234.
8. Ahmed, M. A. K., Fjellvåg, H. and Kjekshus, A. *Acta Chem. Scand. 48* (1994) 537.
9. Werner, P.-E. *Program SCANPI-6*, Institute of Inorganic Chemistry, University of Stockholm, Sweden 1988.
10. Werner, P.-E. *Program TREOR-5*, Institute of Inorganic Chemistry, University of Stockholm, Sweden 1988 [see also *Z. Kristallogr. 120* (1964) 375].
11. Ersson, N. O. *Program CELLKANT*, Chemical Institute, University of Uppsala, Sweden 1981.
12. Pawley, G. S. *Program ALLHKL*, Department of Physics, Edinburgh University, UK 1981 [see also *J. Appl. Crystallogr. 14* (1981) 357].
13. Altomare, A., Cascarono, G., Giacovazzo, C., Guagliardi, A., Burla, M. C., Polidori, G. and Camalli, M. *Program SIRPOW92*, Dip. Geomineralogico, University of Bari, Italy 1992.
14. Wiles, D. B., Sakthivel, A. and Young, R. A. *Program DBW3.2S*, School of Physics, Georgia Institute of Technology, Atlanta, GA 1988 [see also Wiles, D. B. and Young, R. A. *J. Appl. Crystallogr. 14* (1981) 149].
15. de Wolff, P. P. *J. Appl. Crystallogr. 1* (1968) 108.
16. Brese, N. E. and O'Keeffe, M. *Acta Crystallogr. Sect. B 47* (1991) 192.
17. Furuseth, S., Selte, K., Hope, H., Kjekshus, A. and Klewe, B. *Acta Chem. Scand., Ser. A 28* (1974) 71.
18. Fjellvåg, H. and Kjekshus, A. *Acta Chem. Scand. 48* (1994) 815.
19. Thomas, P. A., Glazer, A. M. and Watts, B. E. *Acta Crystallogr., Sect. B 46* (1990) 333.
20. Protas, J., Marnier, G., Boulanger, B. and Menaert, B. *Acta Crystallogr., Sect. C 45* (1989) 1123.
21. Mrose, M. E. *Am. Mineral. 46* (1961) 146.

Received April 6, 1995.